ISSN 2070-2051, Protection of Metals and Physical Chemistry of Surfaces, 2010, Vol. 46, No. 4, pp. 438–443. © Pleiades Publishing, Ltd., 2010.
Original Russian Text © A.A. Solov'eva, N.S. Sochugov, K.V. Oskomov, N.A. Zaharov, 2010, published in Fizikokhimiya Poverkhnosti i Zashchita Materialov, 2010, Vol. 46, No. 4, pp. 361–366.

NANOSCALE AND NANOSTRUCTURED MATERIALS AND COATINGS

Properties of Multilayer ZnO:Ga/Ag/ZnO:Ga Coatings Applied by Magnetron Sputtering

A. A. Solov'ev, N. S. Sochugov, K. V. Oskomov, and N. A. Zaharov

[a] *Institute of Strong Current Electronics, Siberian Division, Russian Academy of Sciences, 2/3 Akademicheskii prosp., Tomsk, 634055 Russia*

e-mail: andrewsol@mail.ru

Received March 16, 2009

Abstract—The methods of van der Pau, spectrometry, and atomic force microscopy were used to study the optical and electrophysical properties of multilayer ZnO:Ga/Ag/ZnO:Ga coatings applied by magnetron sputtering. The effect of the thickness of the coating layer was studied with respect to the surface resistance, transparency, and reflection of the multilayer structure in the visible and infrared wavelength ranges. The coating surface morphology and moisture resistance was studied. The ZnO:Ga/Ag/ZnO:Ga coatings were shown to have a high transparency (T = 90%) in the visible range, high reflection coefficient in the IR range (R = 93%), and low surface resistance (R_s = 4.88 Ohm/sq). The moisture resistance studies showed the highest moisture resistance of ZnO:Ga (25 nm) / Ag (15 nm) / ZnO:Ga (75 nm) coatings, which are not changed by testing and can be used for the effective protection of silver films against degradation.

DOI: 10.1134/S2070205110040088

INTRODUCTION

The ultrafine (nanoscale) metal (Au, Ag, Cu) films are widely used in various sciences and technologies due to their unique properties, which are not typical for bulk materials [1, 2]. Silver films are used, inter alia, as the basic functional layer in multilayer low-emission coatings. However, we know that silver films are unstable in humid atmosphere, where they start to degrade with worsening electrical and optical properties. Moisture was shown to strengthen the migration of silver atoms in the film brought to agglomeration. For this reason, low-emission silver coatings with dielectric–silver–dielectric structure should be carefully packed with desiccants in the course of storage or transportation [3]. Therefore, it is important to study the increasing resistance of Ag films to degradation. For example, as was suggested in [4], for lower surface roughness and higher adhesion and resistance, we applied silver films by ionic assistance. The films applied by an electron beam evaporation together with ion beam surface bombardment at a current density of 10 mcA/cm^2 were shown to have a more compact structure that prevents the penetration of water vapors into the film.

As was suggested in [5], the thermal stability of silver films is strongly affected by the substrate properties. Thus, if applied to the ZnO substrate (2–3 nm thick), silver films had preferential orientation in the plane of the most compact packing (111). They were also characterized by significantly fewer agglomerates that arise on the film surface due to the diffusion of silver atoms than in the case of a coating consisting of stochastically oriented grains. It is considered that the nucleation sites of the formed agglomerates are interfaces of film grains [6]. Other authors [7] found that Ag films applied to ZnO substrate are more stable to moisture degradation. For higher corrosion strength, silver is often alloyed with Au, Pd, Pt, Cu, or other metals [8] or buffer metal layers (Ti, etc.) of subnanometer thickness (~2 nm) are applied between the layers of silver and dielectric [9]. Our earlier studies [10, 11] showed that silver films applied to glass substrates by AC magnetron sputtering become continuous and fairly compact with thicknesses of about 8 nm. However, the use of pulse magnetron sputtering enables one to significantly improve the quality of the applied films. Pulse-current applied films with the same thickness have better texture, higher IR reflection coefficient and density of structure, and lower specific resistance and surface roughness. Using this method, we produced continuous silver films with thicknesses of 4 nm and surface roughness of 0.52 nm. Therefore, in this work, silver films were applied by pulse magnetron sputtering at a frequency of 40 kHz and relative pulse duration of 50%.

This work was targeted to study the structure of ultrafine silver films produced by pulse magnetron sputtering, their degradation rates in free condition and in the multilayer structure of MeO_x/Ag/MeO_x low-emission coating, as well as methods of the purposeful deceleration and suppression of this process. We selected transparent gallium alloyed zinc oxide as the oxide layer material. This alloyed zinc oxide has lower specific resistance and better optical properties than fluorine alloyed tin oxide. Recently the optical and electrophysical properties of zinc oxide were signifcantly improved and it was considered to be a real alternative for replacing expensive In-Sn oxide (ITO) coatings.

Application parameters of ZnO : Ga/Ag/ZnO : Ga multilayer coatings

Material	Pressure, Pa	Discharge voltage, V	Discharge current, A	Discharge power, W	Power mode	Specimen rotation speed, rpm
ZnO	0.2	320	0.37	120	DC	2.5
Ag	0.1	650	0.65	430	$f = 40$ kHz	10

EXPERIMENTAL

The coatings were applied in a set with a vacuum chamber made of stainless steel and having the dimensions of 600 × 600 × 600 mm. In addition to the evacuation system based on a turbomolecular pump, the sputtering set was equipped with two magnetron sputtering systems (to apply silver and oxide layers), an ion generator with closed electron drift (for prior plasma ion substrate cleaning), two ApEI-M power sources for magnetron sputtering systems, and ApEI-IS power source for ion generator. The magnetron design and plasma characteristics were described in [12]. The magnetron cathodes were disks (Ag and ZnO : (3.5% at/at) Ga_2O_3 with diameters of 100 mm and thicknesses of 6 mm. Silver was sputtered in the pulse mode at the frequency of 40 kHz and ZnO:Ga_2O_3 ceramic target was sputtered in the DC mode. The arc control system of the magnetron power sources provided an arc energy release that did not exceed 50 mJ.

The ZnO:Ga/Ag/ZnO:Ga coatings were applied by layers of zinc oxide and silver. Here, the thickness of each layer was regulated by the sputtering time. The coatings were applied at room temperature to 4 mm M0 architectural glass substrates. For uniform coatings to be applied along the substrate, the latter was rotated around the vacuum chamber axis. The distance between the substrate and magnetron was 130 mm. The coating transparency in the visible wavelength range (400–800 nm) was measured with a USB 2000-VIS-NIR spectrometer. The coating reflection coefficient in the IR wavelength range was measured with an IKS-29 spectrophotometer at the wavelength of 8 μm.

The film thickness was measured with a Solver P47 atomic force microscope. A step was made between the film and substrate by partial removal of the coating. Then, the atomic force microscopy produced the film relief and substrate pattern. The film thickness was assumed as the height of this step. The surface resistance of the produced coatings was measured by the van der Pau method in 0.61 T magnetic film at the room temperature. The test specimen dimensions were 17 × 17 mm.

RESULTS AND DISCUSSION

The goals of this work included the degradation studies of silver films placed for protection from atmospheric factors between gallium alloyed zinc oxide layers. Because they were formed by ZnO:Ga_2O_3 cathode sputtering in argon atmosphere, there was no need in application of any buffer layers protecting silver from oxidation. The coating conditions are represented in Table 1. We produced a series of ZnO:Ga/Ag/ZnO:Ga coatings with ZnO:Ga layer thickness of 25 or 50 nm and Ag layer thickness was 1.5–18 nm.

The surface resistance of the multilayer coating is lower for thinner silver layers (Fig. 1). If the Ag layer is 4.5 nm thick, the coating surface resistance is high, evidencing discontinuous coating. For Ag layer of 15 nm and thicker, the surface resistance decreases to 4 Ohm/sq, then changes insignificantly. Apparently, a complete Ag film is formed at the thickness of 10–12 nm because the surface resistance sharply increases below this level. As follows from these results, ZnO:Ga layers produce the minimum effect to the electrical characteristics of the whole multilayer structure, whose conductivity is determined primarily by the conductivity of Ag layer.

At a thicker silver layer, the coating transparency decreases in the visible wavelength range and the reflection coefficient increases in the IR range. Figure 2 represents the ZnO:Ga/Ag/ZnO:Ga coating transparency at the wavelength of 550 nm vs. silver layer thickness.

We know that, like most metal coatings, silver films start to grow from islets, which grow and associate into closed chains and the network structure, and, finally,

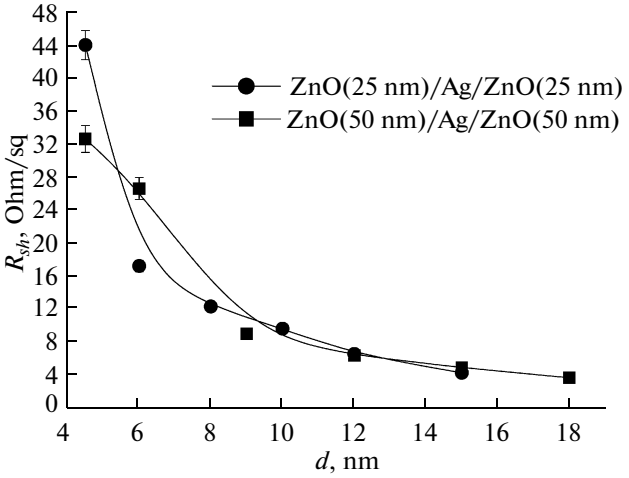

Fig. 1. Surface resistance R_{sh} of ZnO:Ga/Ag/ZnO:Ga coatings vs. silver layer thickness d.

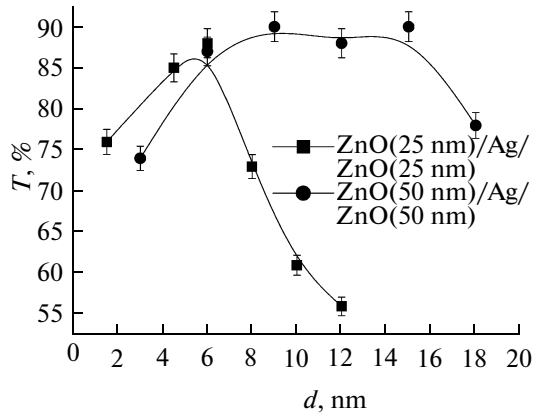

Fig. 2. Transparence T of ZnO:Ga/Ag/ZnO:Ga coatings vs. silver layer thickness d ($\lambda = 550$ nm).

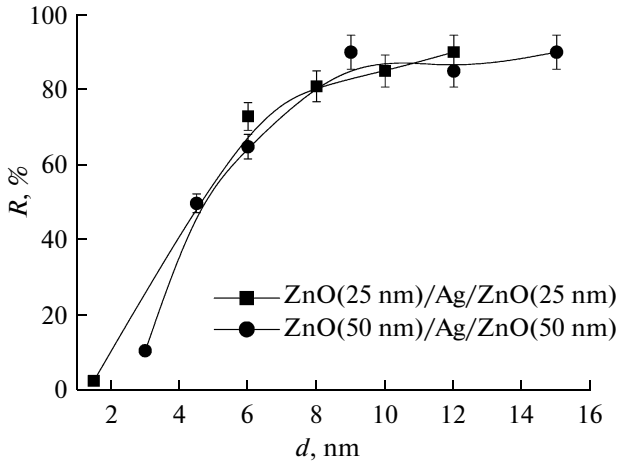

Fig. 3. Reflection coefficient R of ZnO:Ga/Ag/ZnO:Ga coatings vs. silver layer thickness d ($\lambda = 8$ μm).

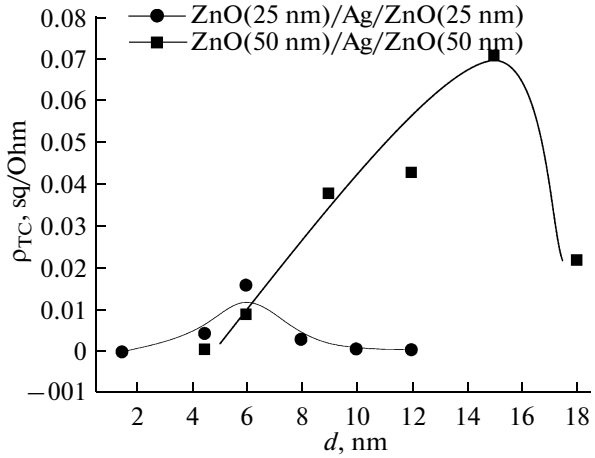

Fig. 4. FOM ρ_{TC} of ZnO:Ga/Ag/ZnO:Ga coatings vs. silver layer thickness d.

make the continuous films [13]. When the film formation takes place at the stage of islets, light transmission through the coating weakens due to scattering on these islets. However, the transparency of the coating is still high and the IR reflection coefficient is low. Along with the increasing area occupied by the growing film islets, the system transparency in the visible wavelength range sharply decreases and the IR reflection coefficient sharply decreases. At the stage of coalescence of islets and formation of continuous film, its transparency is 85–90% and the IR reflection coefficient is 90–95%. For a thicker film, the light scattering effect to transparency and IR reflection decreases and these parameters tend to 0 and 100%, respectively.

Figure 2 shows that the ZnO:Ga/Ag/ZnO:Ga multilayer coating transparency depends on the thickness of both silver and oxide layers. There is a characteristic Ag layer thickness, where the transparency of the ZnO:Ga/Ag/ZnO:Ga coating is maximum. Apparently, the maximum coating transparency is achieved when the silver layer thickness corresponds to the formed continuous film thickness. The transparency of thinner or thicker films is lower due to light scattering on islets or higher reflection of Ag layer, respectively. For the ZnO:Ga layers of 25 nm thick, the coating has the highest transparency at the Ag layer of 6 nm thick. However, for 50-nm-thick oxide layers, the coating is most transparent at an 8–15-nm-thick Ag layer. Here, the range of the thickness of the Ag layer is wider for the maximum transparency (~90%) of the multilayer coating.

As follows from the reflection coefficient of the ZnO:Ga/Ag/ZnO:Ga coating versus the curves of the thickness of the Ag layer (Fig. 3), at a thickness of 9 nm, the reflection coefficient achieves a level of 90%, but hardly changes along with a further increase in thickness. Because the lower resistance of transparent conducting coatings is normally due to thicker coatings with inevitably lower transparency, it is necessary to know the film thickness corresponding to the optimum resistance/transparency ratio.

Transparent conducting coatings with the known transparency and electrical resistance are compared with the figure of merit (FOM, ρ_{TC}) [14, 15]. G. Haake [16] was the first to suggest the use of FOM calculated by the formula $\rho_{TC} = T^{10}/R_s$, where T is the optical transparency of coating in the range of 400–780 nm and R_s is the surface resistance. In the case of a ZnO:Ga/Ag/ZnO:Ga multilayer coating, FOM enables one to find the Ag and ZnO:Ga layer thicknesses by providing the best combination of optical and electrical properties of the structure in general.

Figure 4 shows ρ_{TC} vs. layer thickness in ZnO:Ga/Ag/ZnO:Ga coating. As we see in these curves, if the oxide layer thickness increases from 25 to 50 nm, the optimum Ag layer thickness increases from 6 to 15 nm. Here, the range of Ag layer thicknesses, which provide the maximum ρ_{TC} values, significantly widens. Therefore,

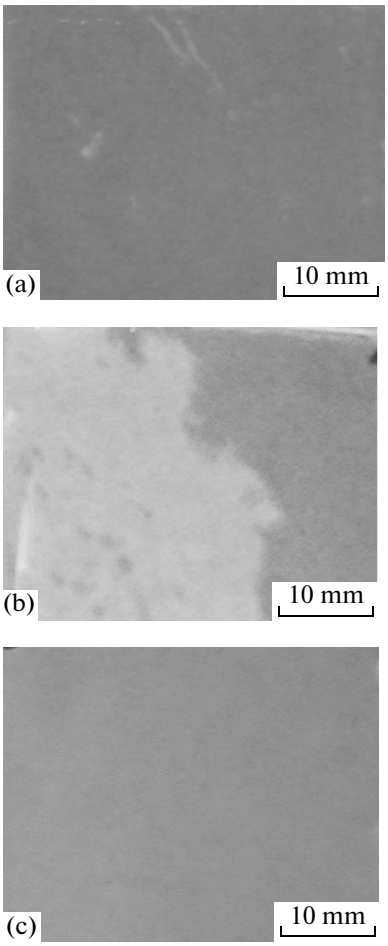

Fig. 5. Appearance of coated specimens after moisture test: (a) Ag (15 nm), (b) ZnO:Ga (25 nm) / Ag (12 nm) / ZnO:Ga (25 nm), (c) ZnO:Ga (25 nm) / Ag (15 nm) / ZnO:Ga (75 nm).

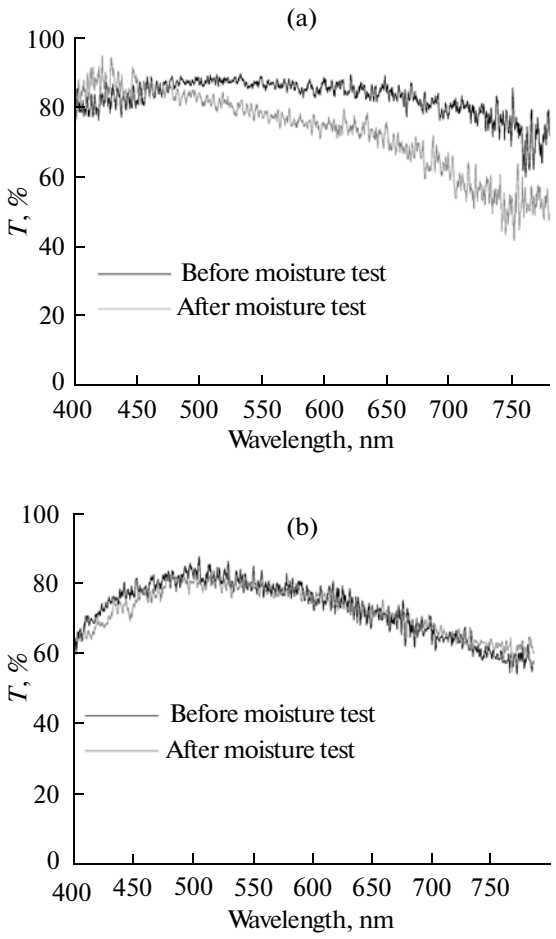

Fig. 6. Transparence of Ag (15 nm) (a) and ZnO:Ga (25 nm) (b).

with respect to the optical and electrical characteristics, the optimum structure is ZnO:Ga (50 nm) / Ag (15 nm) / ZnO:Ga (50 nm), which has the highest transparency T = 90%, reflection coefficient R = 93%, and FOM ρ_{TC} = 0.071, but the lowest surface resistance R_s = 4.88 Ohm/sq.

In order to study the moisture resistance of the produced coatings, we selected the test described in GOST 30733-2000 ("Glass with Low-Emission Solid Coating: Technical Specifications"). Here, the term "solid coating" refers to tin oxide applied by pyrolysis in the course of making float glass (K glass). According to these specifications, coated specimens are placed in a bath with distilled water. Water is heated to a temperature of (100 ± 2)°C, which is maintained for 2 h. After testing, the number and size of defects is measured for each specimen. The rate of degradation of the coating was estimated visually.

Figure 5 represents the appearance of coatings after the moisture test. For comparison, we used 15 nm Ag film applied directly to the glass and ZnO:Ga (25 nm) / Ag (12 nm) / ZnO:Ga (25 nm) multilayer coating. After the moisture test, the Ag film showed few defects (Fig. 5a) and significantly lost the transparency in the wavelength range of 500–800 nm (Fig. 6a). This lower transparency is due to the film agglomeration and light scattering on the formed islets. These changes in the film structure are evidenced by the surface morphological studies carried out by atomic force microscopy before and after the moisture test (Fig. 7). We see that the surface of moisturized Ag film contains much more agglomerates up to 20 nm high formed by the migration of Ag atoms into sphere-like formations with a base diameter of up to 100 nm.

After the moisture test of ZnO:Ga (25 nm) / Ag (12 nm) / ZnO:Ga (25 nm) coating, we found (Fig. 5b) its full peeling and removal in the major part of the specimen surface. Apparently, the outer ZnO:Ga (25 nm) layer does not prevent the penetration of water molecules to silver film. In order to terminate the access of moisture to the Ag layer, the thickness of the outer ZnO:Ga layer was increased to 75 nm, while that of the Ag layer was increased to 15 nm, which decreased the coating transparency to 83%, but increased the coating continuity and

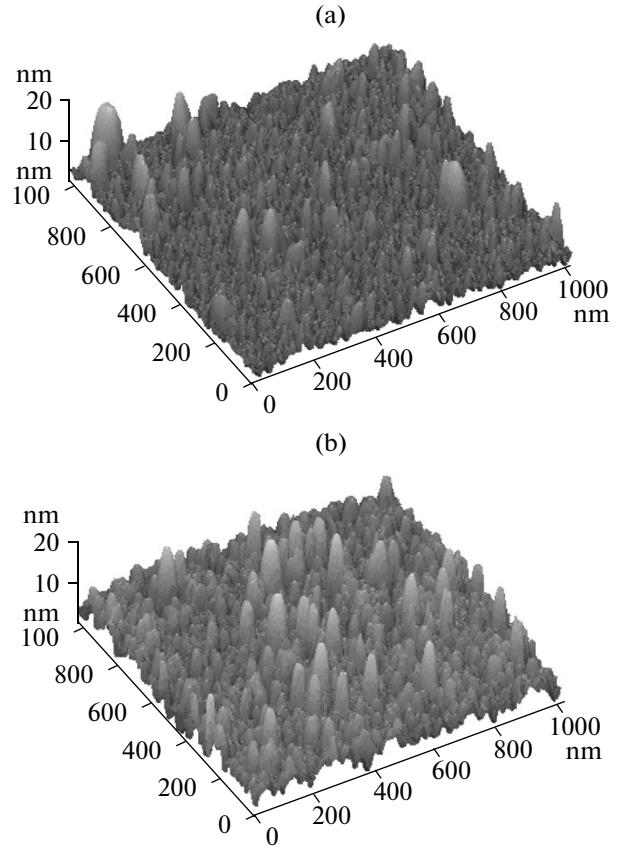

Fig. 7. AFM patterns of 15 nm Ag film on glass substrate before (a) and after (b) moisture test. Scan dimensions 1 μm × 1 μm.

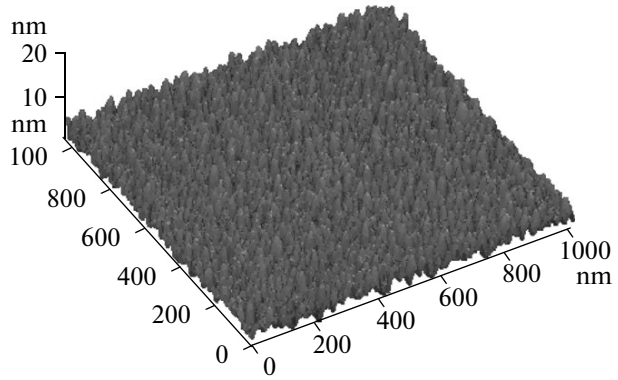

Fig. 8. AFM patterns of ZnO:Ga (25 nm) / Ag (15 nm) / ZnO:Ga (75 nm) coating. Scan dimensions1 μm × 1 μm.

eliminated minor defects that promote the penetration of water to the Ag layer. However, the thickness of the inner ZnO:Ga layer did not change. The moisture tests of ZnO:Ga (25 nm) / Ag (15 nm) / ZnO:Ga (75 nm) coating showed no changes in the tested coating that could be seen by the naked eye (Fig. 5c).

The electrical and optical studies of the given coating showed good reflection capacity (R = 91%) and relatively low surface resistance (R_s = 11.5 Ohm/sq). The transparency measurements before and after the moisture testing showed no changes in the film transparency (Fig. 6b). Our surface morphology studies of ZnO:Ga (25 nm) / Ag (15 nm) / ZnO:Ga (75 nm) coating (Fig. 8) showed that, if the Ag layer is applied to ZnO substrate, the resulting coating has a significantly smoother surface with a grain size of 25–50 nm compared to a single Ag coating of 15 nm (Fig. 7a). This confirms the fact that Ag films applied to ZnO substrate have better quality and higher substrate adhesion, while the surface migration of Ag atoms on this substrate is less strongly expressed.

CONCLUSIONS

1. The electrical and optical characteristics of a ZnO:Ga/Ag/ZnO:Ga multilayer coating were studied. The given characteristics can be regulated by selecting the thicknesses of Ag layer and ZnO:Ga outer layer. The optimum thicknesses of Ag and ZnO:Ga layers were found in the ranges of 12–15 and 50–75 nm, respectively. The coating structure of ZnO:Ga (50 nm) / Ag (15 nm) / ZnO:Ga (50 nm) has the highest FOM (ρ_{TC} = 0.071), high transparency in the visible range (T = 90%), highest reflection coefficient in IR range (R = 93%), and low surface resistance (R_s = 4.88 Ohm/sq).

2. We showed that ZnO:Ga/Ag/ZnO:Ga multilayer structure can be used to increase the corrosion stability of silver films. In the given coating, the first ZnO:Ga layer improves adhesion of Ag layer to the glass substrate, while the second ZnO:Ga layer protects silver from the atmospheric factors. The advantages of this structure are accounted for by the fact that zinc oxide has high moisture resistance and its transparency is fairly high in order to provide the transparency of the multilayer system in general.

3. Our moisture tests showed that ZnO:Ga (25 nm) / Ag (12 nm) / ZnO:Ga (75 nm) coating is most stable to the degradation caused by the effects of moisture.

ACKNOWLEDGMENTS

This work was financially supported by the Russian Foundation for Basic Research (project no. 08-08-99086).

REFERENCES

1. Stearns, M.B., Chang, C.-H., and Stearns, D.G., *J. Appl. Phys.,* 1992, vol. 71, p. 187.
2. Gijs, M. and Bauer, G., *Adv. Phys.*, 1997, vol. 46, p. 285.
3. Ando, E., Suzuki, S., Aomine, N., et al., *Vacuum*, 2000, vol. 59, p. 792.
4. Lee, C.C., Lee, T.Y., and Jen, Y.J., *Thin Solid Films*, 2000, vol. 359, p. 95.
5. Arbab, M., *Thin Solid Films,* 2001, vol. 381, p. 15.

6. Sharma, S.K. and Spitz, J., *Thin Solid Films,* 1980, vol. 65, p. 339.
7. Ando, E. and Miyazaki, M., *Thin Solid Films,* 2001, vol. 392, p. 289.
8. Fukuda, S., Kawamoto, S., and Gotoha, Y., *Thin Solid Films*, 2003, vol. 442, p. 117.
9. Chiba, K., Takahashi, T., Kageyama, T., and Oda, H., *Appl. Surf. Sci.*, 2005, vol. 246, p. 48.
10. Soloviev, A.A., Sochugov, N.S., and Oskomov, K.V., *Izv. Vyssh. Uchebn. Zaved., Fiz.*, 2007, no. 9, p. 453.
11. Soloviev, A.A., Sochugov, N.S., and Oskomov, K.V., *Izv. Vyssh. Uchebn. Zaved., Fiz.*, 2007, no. 9, p. 394.
12. Solov'ev, A.A., Sochugov, N.S., Oskomov, K.V., and Rabotkin, S.V., *Fiz. Plazmy*, 2009, vol. 35, no. 4, p. 1 [*Plasma Phys. Rep.* (Engl. Transl.), vol. 35, no. 4, p.].
13. Sun, X., Hong, R., Hou, H., et al.,*Thin Solid Films,* 2007, vol. 515, p. 6962.
14. Sahu, D.R. and Huang, J.-L., *Thin Solid Films*, 2006, vol. 515, p. 876.
15. Mohamed, S.H., *J. Phys. Chem. Solids*, 2008, vol. 69, p. 2378.
16. Haacke, G., *J. Appl. Phys.*, 1976, vol. 47, p. 4086.